



HHS Public Access

Author manuscript

Angew Chem Int Ed Engl. Author manuscript; available in PMC 2015 April 27.

Published in final edited form as:

Angew Chem Int Ed Engl. 2010 November 15; 49(47): 8876–8879. doi:10.1002/anie.201003900.

Urothermal Synthesis of Crystalline Porous Materials

Dr. Jian Zhang,

Department of Chemistry and Biochemistry, California State University, Long Beach, CA 90840,
Fax: (+) 562-985-8557. Fujian Institute of Research on the Structure of Matter, Chinese Academy
of Sciences, Fuzhou, China 350002

Julia T. Bu,

Department of Chemistry, University of California, Riverside

Dr. Shumei Chen,

Department of Chemistry and Biochemistry, California State University, Long Beach, CA 90840,
Fax: (+) 562-985-8557

Tao Wu,

Department of Chemistry, University of California, Riverside

Dr. Shoutian Zheng,

Department of Chemistry and Biochemistry, California State University, Long Beach, CA 90840,
Fax: (+) 562-985-8557

Yigang Chen,

Department of Chemistry and Biochemistry, California State University, Long Beach, CA 90840,
Fax: (+) 562-985-8557

Ruben A. Nieto,

Department of Chemistry and Biochemistry, California State University, Long Beach, CA 90840,
Fax: (+) 562-985-8557

Prof. Dr. Pingyun Feng, and

Department of Chemistry, University of California, Riverside

Prof. Dr. Xianhui Bu

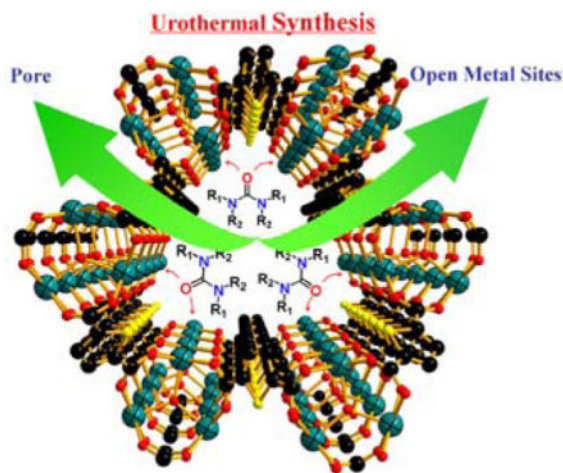
Department of Chemistry and Biochemistry, California State University, Long Beach, CA 90840,
Fax: (+) 562-985-8557

Xianhui Bu: xbu@csulb.edu

Abstract

Correspondence to: Xianhui Bu, xbu@csulb.edu.

Supporting information for this article is available on the WWW under <http://www.angewandte.org> or from the author.



Pores from Urea Urea derivatives are shown here to be a highly versatile solvent system for the synthesis of crystalline solids. In particular, reversible binding of urea derivatives to framework metal sites has been utilized to create a variety of materials integrating both porosity and open-metal sites.

Keywords

metal-organic frameworks; microporous materials; solvents; ionothermal synthesis; solvothermal synthesis

The intensive research in past several decades has resulted in the synthesis of porous materials with diverse chemical compositions and framework topologies.^[1] Still, the search for new porous materials continues to be a highly active field because of their potential applications in emerging areas such as gas storage^[2], CO₂ capture^[3], and catalysis^[4].

Porous materials are usually synthesized under relatively low temperatures (<200°C), which necessitates the use of solvents to promote the diffusivity of reactants and to grow crystals of suitable sizes. In fact, solvents have played vital roles in the development of different families of porous materials. For example, inorganic porous materials such as zeolites are often synthesized using hydrothermal method, even though non-aqueous synthesis has also been explored.^[5] On the other hand, recently developed metal-organic frameworks (MOFs) often rely on the use of organic solvents such as DMF in a process called solvothermal synthesis. It is worth noting that solvothermal synthesis is an overly broad concept, covering solvents with dramatically different structures and properties. As such, it generally conjures up little correlation between solvents used and structural features or properties of materials prepared in them. With the recent advance in the understanding of correlations between structures and properties, it has become increasingly desirable to design synthetic methods to target specific structural features and physical or chemical properties.

In this work, we explore a versatile synthesis method (denoted as urothermal synthesis here) based on the use of various urea derivatives as solvents. One highly useful feature of urothermal synthesis is the reversible bonding of urea derivatives to metal sites, which

allows them to competitively bond to framework metal sites and yet in many cases they can be easily removed after crystallization to generate both porosity and open metal sites. The competition for coordination to metal sites among urea derivatives and against other solvents such as DMF or DEF is an interesting aspect of this synthetic process and can also be utilized to provide additional structural control.

Prior to this work, urea and urea derivatives were rarely used as solvents for the synthesis of MOFs. However, as a well-known component in deep eutectic solvents, urea and urea derivatives have contributed to the ionothermal synthesis of interesting porous materials, sometimes through decomposition to generate amine templates.^[6]

The large variety of urea derivatives, together with various organic crosslinking ligands and metal ions create numerous synthetic possibilities, as shown by many new materials prepared in this work (Tables 1 and S1). These materials comprise various organic ligands (Scheme S1), many metal ions, and five symmetrical urea derivatives (two with N-H groups and three without) (Scheme 1). For comparative purposes, one cyclic and two acyclic amide solvents, DMF, DEF, and 2-pyrrolidinone (pyrol), are also studied.

These new structures reveal that the major interaction between urea derivatives and framework metal sites is the coordinate interaction between carbonyl oxygen and metal ions (i.e., -C=O-M), supplemented, in some cases, by H-bonding interaction between N-H containing urea derivatives and the oxygen of the carboxyl group. Some urea derivatives such as tm-urea, e-murea, and p-murea, (Scheme 1) have no N-H groups and therefore can not form N-H...O type H-bonds. As shown below, the formation of H-bonding is one of the factors that affect the bonding affinity of urea derivatives to the framework metal sites.

Compounds **1** to **5**, based on the Y-bdc (bdc = 1,4-benzene-dicarboxylate) system, provide an excellent illustration of the roles of urea derivatives, especially the competitive bonding nature of different urea derivatives in relation to common solvents such as DEF. Even though Y³⁺ sites in as-synthesized crystals in **1-5** are 8-coordinate (two of which are two solvent molecules and are potential open-metal sites, Fig. S1), **1-5** exhibit the same 4-connected moganite (denoted: **mog**) topology by reducing the Y³⁺ sites as 4-connected nodes (Fig. 1a–b). The difference among **1-5** is in the type of the pendent ligand attached to the framework (Fig. S1). Therefore, compounds **1-5** make it possible to probe ligand affinity to metal sites by keeping other structural features the same.

Compound **2**, made by using only e-urea hemihydrate as the solvent, illustrates dual interactions (-C=O-M and N-H...O) between urea derivatives and the framework. In **2**, two crystallographic independent e-urea ligands are coordinated to one Y³⁺ site and are situated inside the rectangular channel along the *a* axis (Fig. 1b). Each e-urea ligand forms one N—H...O H-bond with one carboxylate O atom of the framework and the N...O distances are 2.769 Å and 2.990 Å, respectively, suggesting the different H-bonding strength. The e-urea associated with the weaker H-bond can be replaced by competing solvent molecules when the synthesis is performed in a mixed solvent, leading to the synthesis of **3** to **5**.

Compounds **3-5**, prepared from a mixed solvent system, allow us to compare the bonding affinity of different solvent molecules to the metal sites. Thus, the different combination of

various solvents, e-urea with p-murea (**3**), e-urea with DEF (**4**), and e-urea with DMF (**5**), leads to three framework structures (**3-5**) similar to **2**. However, both types of solvent molecules were incorporated as the pendent ligands. Half of the e-urea ligands in **2**, which have weaker H-bonds to the framework, are replaced by p-murea in **3**, DEF in **4**, and DMF in **5**, respectively (Fig. S1).

To further probe the bonding affinity, we also explored the tri-component solvent system. In the case of e-urea/p-murea/DEF, **4** (instead of **3**) containing e-urea and DEF is formed. This shows that as far as the moganite topology is concerned, p-murea has a weaker affinity than e-urea and DEF. In **1-5**, the consistent formation of the **mog**-type frameworks is likely dictated by the strong structure-directing role of e-urea through its combined -C=O-M and N-H...O interactions.

The difference between **1** and **2** shows the effects of reaction temperature and ligand size. By using the same reaction condition as **2**, except with an increase of the temperature from 120 to 140 °C, half of e-urea molecules in **2** are replaced by H₂O, leading to the formation of **1**. Even though **1** has the same mog topology as **2-4**, it has 2-fold interpenetration (Fig. 1a), likely caused by small size of H₂O. This suggests that the 2-fold interpenetration in **1** is eliminated by replacing H₂O with larger solvent molecules, such as e-urea in **2**, p-murea in **3**, DEF in **4**, and DMF in **5**.

What will happen if e-urea, which favors the mog topology, is not used? Again, we focus on the Y-bdc system so that the solvent effect can be highlighted. Reactions between Y³⁺ ions and bdc in three solvent systems (DEF; DEF with p-urea; and pyrol) generate three new structures (**6-8**) in which the Y³⁺ ions are bridged by carboxylate groups of bdc ligands into chains (Fig. S1f-h) that are further crosslinked by benzene rings of the bdc ligands to generate the 3D framework (Fig. 1c-d). The solvent molecule in **6-8** is attached to Y³⁺ to complete its coordination geometry (Fig. S1f-h). Two different (4,6)-connected topologies were observed. In **6**, the distribution of solvent molecules (DEF) along the Y-BDC chain follows the UUDDUUDD... pattern (U = up, D =Down), resulting in a (4,6)-connected trinodal net. In **7** (p-urea) and **8** (pyrol), the UDUDUD... pattern is observed, leading to another type of net.

The synthesis of p-urea-containing **7** from the mixed DEF and p-urea solvent further highlights the competitive bonding of ligands to the framework and confirms the significance of integrated metal-ligand and H-bonding interactions in enhancing the affinity of N-H-containing urea derivatives to the framework. When used alone, DEF is readily incorporated into **6**. However, when p-urea is used together with DEF, compound **7** which contains only p-urea is formed, even though the molar ratio of 5:1 between DEF and p-urea in the synthesis mixture is in favor of DEF.

It is also of interest to compare **2** and **8**, which are made from e-urea and pyrol, respectively. These two ligands have the similar size and shape, except that e-urea has -NH group on both sides of -C=O group whereas pyrol has a -NH group at only one side. Such a difference is, however, sufficient to generate two different framework topologies.

The urothermal synthesis shown above for the Y-bdc system can be extended to many metal ions including lanthanides (Ln), transition metals, and even alkali and alkaline-earth metals, demonstrating the versatility of the method. A series of Ln-bdc compounds were synthesized by reacting Ln^{3+} salts with H_2bdc in e-urea semihydrate solvent at 140 °C. Topologically, these new Ln-bdc phases are either isostructural to the Y^{3+} compound **1** (**1a-g** in Table S1) or **2** (**2a-c**), and $\text{Sm}(\text{bdc})_{3/2}(\text{e-urea})$ obtained from deep eutectic solvents (**9**, **9a-b**),^[6h] or exhibit new crystalline structures (**20-30**, See Table S1 for details). Furthermore, reactions of d-block metal ions (including Group 12) with bdc also yielded a number of new phases (**40-45**, Tables 1 and S1). For example, the assembly of Co^{2+} or Cd^{2+} with bdc in tm-urea generated two 3D open-frameworks (**URO-44** and **-45**) with 1D channels (Fig. 2c-d). In both frameworks, the tm-urea solvent molecules are located within the channels and serve as the templates (as compared to pendent ligands in **1-9**).

We have so far exclusively used the bdc ligand in order to focus on roles of different urea derivatives. Clearly, the urothermal synthesis works with other crosslinking ligands too (Scheme S1 and Table S1). Three notable examples are **URO-123**, **URO-160**, **Zn/BTB-tsx-pyrol** (BTB = 1,3,5-benzenetricarboxylate). **URO-123** based on 1,2,4-benzenetricarboxylate and Zn^{2+} possesses a chiral microporous framework with large rectangular channels along the *a* axis (Fig. 2b), while **URO-160** constructed from thiophene-2,5-dicarboxylate is an anion (NO_3^-) templated porous framework with exposed Yb_3O trimeric units (Fig. 2a). In **Zn/BTB-tsx-pyrol** which is related to Zn/BTB-tsx reported earlier,^{1g} an interesting feature is that there are two pyrol ligands attached to each Zn_4O unit. Furthermore, previously reported highly porous materials can also be made. For example, **U-MOF-177** (Table S1) has been made by using p-murea/ H_2O as the solvent, instead of DEF originally used for synthesizing MOF-177.^{1b}

Frameworks consisting of Li^+ ions are quite rare, in part because of the high solvation energy of Li^+ . Thus it is of particular interest to develop new solvent systems for making lithium frameworks. As an example of the relevance of the urothermal synthesis to the preparation of Li framework structures, **URO-511** was synthesized by using e-murea (Fig. 2e).

A particularly interesting finding is the reaction of D-camphoric acid with ethyleneurea to generate a new enantiopure ligand (L1) found in **URO-502** (Fig. 2f-g), demonstrating that the versatility of the urothermal method extends beyond the synthesis of crystalline porous materials to include unusual organic transformations.

Thermal gravimetric analysis indicates that Y-bdc compounds (**1-4**, **6**, **8**) exhibit a sharp weight loss upon solvent removal between 200–300 °C and remain stable until about 500°C (Fig. S11). After heating **2** to **4** at 250 °C for 10 minutes, powder X-ray diffraction shows that samples **2** to **4** have the same pattern before and after the heating, confirming that they are stable towards the solvent loss (Fig. S14). Volumetric gas adsorption measurements (N_2 , H_2 and CO_2) for select samples were also performed. The samples of **1**, **2**, **6** and **URO-123** were degassed at 200 °C prior to the measurement. The N_2 adsorption/desorption studies of **1**, **2**, **6** and **URO-123** reveal that all of them are porous (Figs. S11–S13). BET and Langmuir surface areas for each sample are summarized in Table S2, together with the H_2 adsorption

results at 77 K and 1 atm and the CO₂ adsorption results at 273K and 1 atm. The porosity values shown by these materials (Langmuir surface areas from 198 to 300cm³/g) demonstrates that the promise of urothermal synthesis goes beyond just the creation of diverse structural types to include the generation of porosity.

In conclusion, we demonstrate here that urothermal synthesis, based on the use of urea derivatives as solvents, offer promise for the synthesis of a wide range of crystalline materials. In particular, we show that the method is well suited for the creation of crystalline porous materials through the reversible binding of urea-type ligands to framework metal sites. It is expected that further refinement of urothermal method will have a great potential for the creation of novel porous materials with possible applications.

Supplementary Material

Refer to Web version on PubMed Central for supplementary material.

Acknowledgments

We thank the support of this work by NSF (X. B. DMR-0846958, P. F. CHEM-0809335.), DOE (P. F. DE-SC0002235), and Research Corporation (X.B. CC6593). X. B is a Henry Dreyfus Teacher Scholar.

References

1. a) Cheetham AK, Ferey G, Loiseau T. *Angew Chem.* 1999; 111:3466. *Angew Chem Int Ed.* 1999; 38:3268. b) Chae HK, Siberio-Perez DY, Kim J, Go Y, Eddaoudi M, Matzger AJ, O'Keeffe M, Yaghi OM. *Nature.* 2004; 427:523. [PubMed: 14765190] c) Ferey G. *Chem Soc Rev.* 2008; 37:191. [PubMed: 18197340] d) Horike S, Shimomura S, Kitagawa S. *Nature Chemistry.* 2009; 1:695. e) Chen B, Xiang S, Qian G. *Acc Chem Res.* 2010; 43:1115. [PubMed: 20450174] f) Serre C, Mellot-Draznieks C, Surble S, Audebrand N, Fillinchuk Y, Ferey G. *Science.* 2007; 315:1828. [PubMed: 17395825] g) Caskey SR, Wong-Foy AG, Matzger AJ. *Inorg Chem.* 2008; 47:7751–7756. [PubMed: 18672874]
2. a) Morris RE, Wheatley PS. *Angew Chem.* 2008. *Angew Chem Int Ed.* 2008; 47:4966. b) Murray LJ, Dinca M, Long JR. *Chem Soc Rev.* 2009; 38:1294. [PubMed: 19384439] c) Ma S, Zhou H. *Chem Commun.* 2010; 46:44. d) Pan L, Sander MB, Huang X, Li J, Smith M, Bittner E, Bockrath B, Johnson JK. *J Am Chem Soc.* 2004; 126:1308. [PubMed: 14759166]
3. a) Millward AR, Yaghi OM. *J Am Chem Soc.* 2005; 127:17998. [PubMed: 16366539] b) Banerjee R, Phan A, Wang B, Knobler C, Furukawa H, O'Keeffe M, Yaghi OM. *Science.* 2008; 319:939. [PubMed: 18276887]
4. a) Bradshaw D, Claridge JB, Cussen EJ, Prior TJ, Rosseinsky MJ. *Acc Chem Res.* 2005; 38:273. [PubMed: 15835874] b) Ma L, Abney C, Lin W. *Chem Soc Rev.* 2009; 38:1248. [PubMed: 19384436] c) Lee JY, Farha OK, Roberts J, Scheidt KA, Nguyen ST, Hupp JT. *Chem Soc Rev.* 2009; 38:1450–1459. [PubMed: 19384447]
5. Morris RE, Weigel SJ. *Chem Soc Rev.* 1997; 26:309.
6. a) Jin K, Huang X, Pan L, Li J, Appel A, Wherland S. *J Chem Soc Chem Commun.* 2002:2872. b) Cooper ER, Andrews CD, Wheatley PS, Webb PB, Wormald P, Morris RE. *Nature.* 2004; 430:1012. [PubMed: 15329717] c) Morris RE. *Chem Commun.* 2009:2990. d) Parnham ER, Morris RE. *Acc Chem Res.* 2007; 40:1005. [PubMed: 17580979] e) Zhang J, Chen S, Bu X. *Angew Chem.* 2008; 120:5342. *Angew Chem Int Ed.* 2008; 47:5434. f) Jhang PC, Yang YC, Lai YC, Liu WR, Wang SL. *Angew Chem Int Ed.* 2009; 48:742. g) Tang MF, Liu YH, Chang PC, Liao YC, Kao HM, Lii KH. *Dalton Trans.* 2007:4523. [PubMed: 17928909] h) Zhang J, Wu T, Chen S, Feng P, Bu X. *Angew Chem.* 2009; 121:3538. *Angew Chem Int Ed.* 2009; 48:3486.

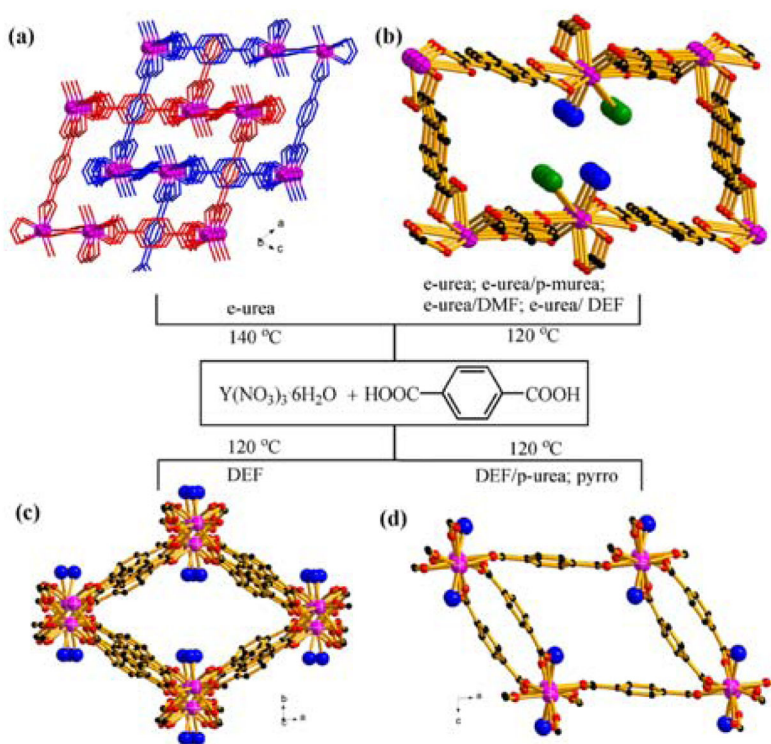


Figure 1. Four different framework types obtained from the self-assembly of $Y(NO_3)_3 \cdot 6H_2O$ and H_2bdc under different solvent conditions or temperatures. (a) 2-fold interpenetrating **mog**-type framework in **1**; (b) non-interpenetrating **mog**-type framework in **2-5**; (c) (4,6)-connected framework in **6**; and (d) (4,6)-connected framework in **7 or 8**. The solvent molecules are shown as blue and green balls (potential open metal sites).

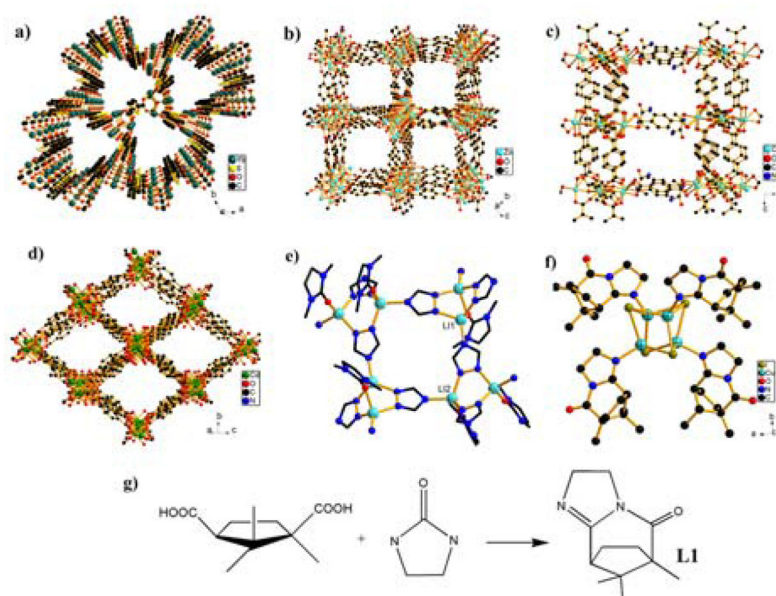
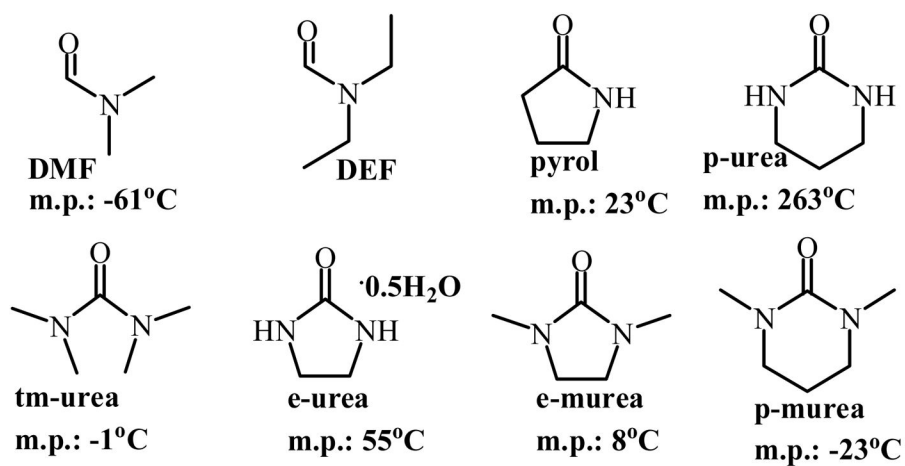


Figure 2. The 3D frameworks of **URO-160** (a), **URO-123** (b), **URO-44** (c) and **URO-45** (d). The coordination environment in **URO-511** (e), the molecular structure of **URO-502** (f), and schematic representation of the in situ synthesis of the enantiopure **L1** ligand in **URO-502** (g).

**Scheme 1.**

The solvents used for synthesis. DMF= dimethylformamide, DEF =diethylformamide, pyrrol = 2-pyrrolidinone, tm-urea = tetramethylurea, e-urea = ethyleneurea, e-murea =1,3-dimethyl-2-imidazolidinone, p-urea = propyleneurea, p-murea = 1,3-dimethyl-propyleneurea.

Table 1

A summary of select materials prepared in this work. For a more complete list of structures with crystallographic data, see Table S1. For structural diagrams of crosslinking ligands, see Scheme S1.

Compounds	Space Group	Additional Roles of Solvents
$Y_2(\text{bdc})_3(\text{e-urea})_2(\text{H}_2\text{O})_2$ (1)	<i>P</i> -1	mixed pendent ligand
$Y_2(\text{bdc})_3(\text{e-urea})_4$ (2)	<i>P</i> -1	pendent ligand
$Y_2(\text{bdc})_3(\text{e-urea})_2(\text{p-murea})_2$ (3)	<i>P</i> -1	mixed pendent ligand
$Y_2(\text{bdc})_3(\text{e-urea})_2(\text{DEF})_2$ (4)	<i>P</i> -1	mixed pendent ligand
$Y_2(\text{bdc})_3(\text{e-urea})_2(\text{DMF})_2$ (5)	<i>P</i> -1	mixed pendent ligand
$Y_2(\text{bdc})_3(\text{DEF})_2$ (6)	<i>C</i> 2/ <i>c</i>	pendent ligand
$Y_2(\text{bdc})_3(\text{p-urea})_2$ (7)	<i>P</i> 2 ₁ / <i>n</i>	pendent ligand
$Y_2(\text{bdc})_3(\text{pyrol})_2$ (8)	<i>P</i> -1	pendent ligand
$[\text{Co}_3(\text{bdc})_3] \cdot (\text{tm-urea})_x$ (URO-44)	<i>C</i> 2/ <i>c</i>	template
$[\text{Cd}_3(\text{bdc})_3(\text{H}_2\text{O})_2] \cdot (\text{tm-urea})_x$ (URO-45)	<i>C</i> 2/ <i>c</i>	template
$\text{Cd}(1,3\text{-bdc})(\text{e-urea})$ (URO-110)	<i>P</i> 2 ₁ 2 ₁ 2 ₁	pendent ligand
$[\text{Zn}_4(\text{OH})_2(1,2,4\text{-btc})_2(\text{H}_2\text{O})] \cdot (\text{p-murea})$ (URO-123)	<i>P</i> 2 ₁ 2 ₁ 2 ₁	template
$\text{Yb}_3\text{O}(\text{thb})_3(\text{p-murea})_3 \cdot (\text{NO}_3)$ (URO-160)	<i>P</i> 31 <i>c</i>	pendent ligand
$[\text{Cd}(\text{thb})(\text{en})_{1/2}(\text{e-urea})] \cdot (\text{e-urea})$ (URO-162)	<i>Pnma</i>	pendent and template
$\text{Cu}_4\text{I}_4(\text{L1})_4$ (URO-502)	<i>C</i> 2	reactant in <i>in-situ</i> ligand formation
$\text{Li}_2(\text{tza})_2(\text{e-murea})_{1.5}$ (URO-511)	<i>P</i> 2 ₁ 2 ₁ 2	pendent ligand